



Supplementary Information for

Antigenic cartography reveals complexities of genetic determinants
that lead to antigenic differences among pandemic GII.4 noroviruses

Authors: Joseph A. Kendra, Kentaro Tohma, Lauren A. Ford-Siltz, Cara J. Lepore, Gabriel I. Parra*

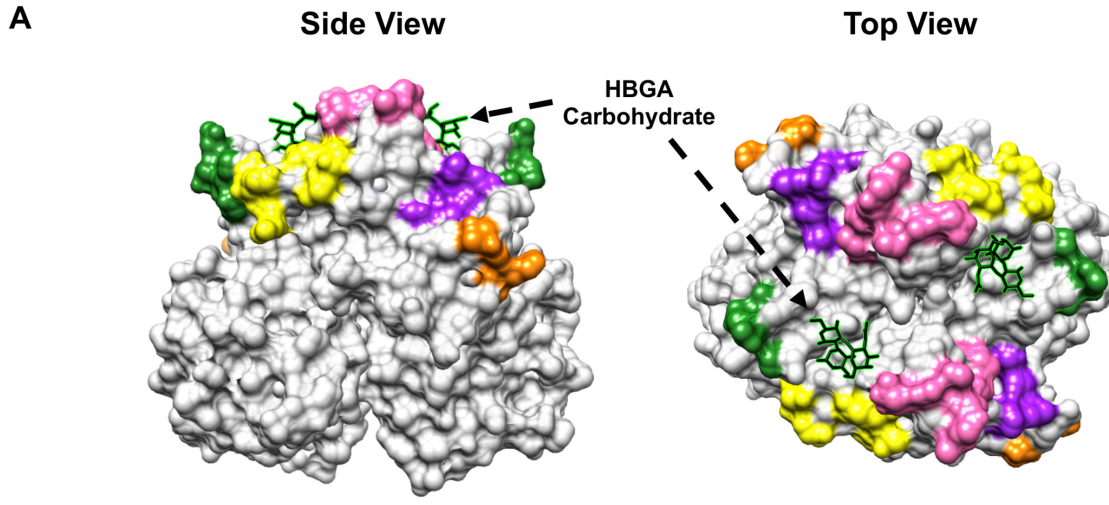
Corresponding Author: Gabriel I. Parra
Email: gabriel.parra@fda.hhs.gov

This PDF file includes:

Figures S1 to S7
Table S1
Legends for Movie S1
Legends for Dataset S1

Other supplementary materials for this manuscript include the following:

Movie S1
Dataset S1



B

	Antigenic Sites																																		
	A							C							D							E							G						
	294	295	296	297	298	368	372	373	339	340	341	375	376	377	378	393	394	395	396	397	407	411	412	413	414	352	355	356	357	359	364				
SY_Arg12866_2014	T	.	.	R	N	E	D	H	.	T	.	.	E	A	N	S	T	T	.	.	S	.	N	T	.	Y	.	A	D	A	R				
SY_NSW0514_2012	T	.	.	R	N	E	D	R	.	T	.	.	E	A	N	G	T	T	.	R	S	.	N	T	.	Y	.	A	D	A	R				
SY_RockvilleD1_2012	T	.	.	R	N	E	D	H	.	T	.	.	E	A	N	S	T	T	.	R	S	.	N	T	.	Y	.	A	D	A	R				
NO_NSW675N_2012	S	.	.	R	N	A	D	.	.	T	.	.	V	.	N	S	T	T	P	R	S	.	N	T	.	Y	.	A	D	S	R				
NO_Virginia_2010	P	.	.	R	N	A	D	.	.	T	N	.	E	.	N	S	A	T	P	R	S	.	N	I	.	Y	.	A	D	S	R				
NO_Ehime2_2009	A	.	.	R	N	A	D	.	.	T	.	.	D	A	N	G	T	A	.	R	S	.	N	T	.	Y	.	A	D	S	R				
AP_Iwate4_2008	T	.	.	R	N	A	D	D	A	N	.	T	A	.	R	S	.	N	S	.	Y	.	A	D	A	R				
OS_Osaka_2007	A	.	.	R	N	A	D	.	.	S	.	.	E	S	.	S	T	T	.	R	L	.	A	D	A	R					
DH_Oregon_2012	A	.	.	R	N	G	E	.	K	R	.	.	E	.	H	S	T	T	.	R	S	.	N	V	.	Y	.	A	D	.	.				
DH_DenHaag89_2006	A	.	.	R	N	S	E	.	K	G	.	.	E	.	H	S	T	T	.	R	S	.	N	V	.	Y	.	A	P	.	.				
DH_Aomori1_2007	A	.	.	R	N	S	E	.	K	G	.	.	E	.	H	G	T	T	.	R	S	.	N	V	P	Y	.	A	P	.	.				
SA_Sakai_2005	P	.	T	R	T	A	D	.	K	G	.	.	E	.	.	S	S	A	.	R	D	.	V	.	.	.	D			
YE_Pune_2006	A	.	T	Q	E	S	S	.	.	R	.	.	E	.	.	S	T	T	.	.	D	.	D	S	.	.	.	N	.	R	.	.			
YE_Yerseke38_2006	A	.	T	Q	E	S	S	.	.	R	.	.	E	.	.	S	T	T	.	.	D	.	D	S	R	.	.			
YE_Kashiwa_2006	A	.	T	Q	E	S	S	.	.	R	.	.	E	.	.	G	T	T	.	.	.	D	S	R	.	.	.			
HT SG4091_2006	A	.	Q	T	S	S	T	.	G	.	.	E	.	.	S	T	T	.	K	S	.	D	S	.	.	A	Y				
HT Nijmegen083_2004	A	.	T	Q	N	S	S	.	.	R	.	.	E	.	.	S	T	T	.	.	D	.	D	S	.	.	I			
HT Cumberland_2004	A	.	T	Q	N	S	S	.	.	R	.	.	E	.	.	S	T	T	.	.	D	.	D	S		
FH_Awa_2004	A	.	T	.	N	N	.	.	K	G	.	.	E	.	.	N	G	T	.	.	S	D			
FH_Oxford_2003	A	.	T	.	N	N	.	.	G	.	.	E	.	.	N	G	T	.	.	S	.	.	.	D	.	.	.	D		
FH_MD2004-3_2004	A	D	T	.	N	N	.	.	G	.	.	E	.	.	N	G	T	.	.	S	.	.	.	D	.	.	.	D		
GR_Matsudo_2002	A	E	S	-	N
GR_Arizona_1996	A	E	.	.	.	A	.	N	-	N
GR_Grimbsy_1995	A	E	N	-	N	I
CA_MD145-12_1987	V	G	S	H	D	T	N	N	R	A	D	F	Q	T	G	D	-	H	H	Q	N	R	T	G	H	S	S	V	H	T	S				

Fig S1. Comparative alignment of historical GII.4 noroviruses shows amino acid changes to antigenic sites. **(A)** Three-dimensional model of the P domain of the norovirus VP1 structural protein. Colors denote the mapped locations of variable antigenic sites A, C, D, E, and G on the P2 subdomain. HBGA carbohydrates are displayed in green. **(B)** Amino acid sequence alignment of antigenic sites for each GII.4 norovirus VLP used in this study. Antigenic site motifs are color coded

for each respective site and the individual residue positions are listed. The sequence from Camberwell MD145-12 1987 (AY032605) was used as the root of this analysis. Dots indicate identical residues to that of the root sequences while letters denote the identity of amino acid change. The structural model of the GII.4 norovirus P domain dimer (Protein Data Bank [PDB] accession number 2OBS) was rendered using UCSF Chimera (version 1.11.2).

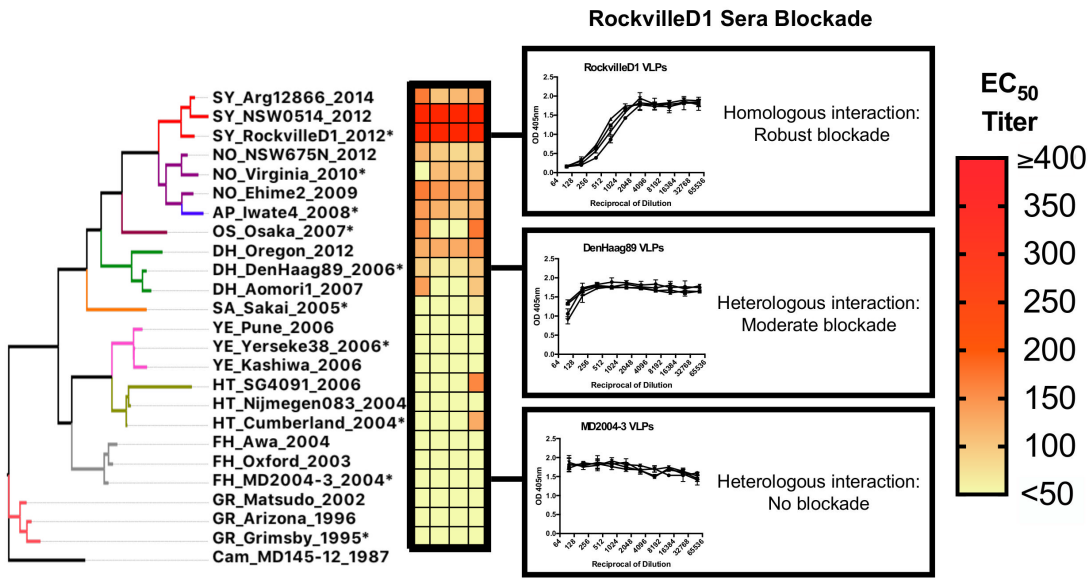


Fig S2. Generalized schematic for HBGA blockade assays against a panel of representative GII.4 VLPs. Summary heat map comparing HBGA blockade profiles of murine hyperimmune sera raised against SY_RockvilleD1 2012 VLP. Specific blockade interactions with the following VLPs are displayed: SY_RockvilleD1 2012 (homologous interaction, strong blockade), DH_DenHaag89 2006 (heterologous interaction, moderate blockade) and FH_MD2004-3 2004 (heterologous interaction, no blockade). Assays were conducted with sera from four different mice as biological replicates run as technical duplicates. VLP blockade activity is presented as OD 405 measurements across two-fold sera dilutions.

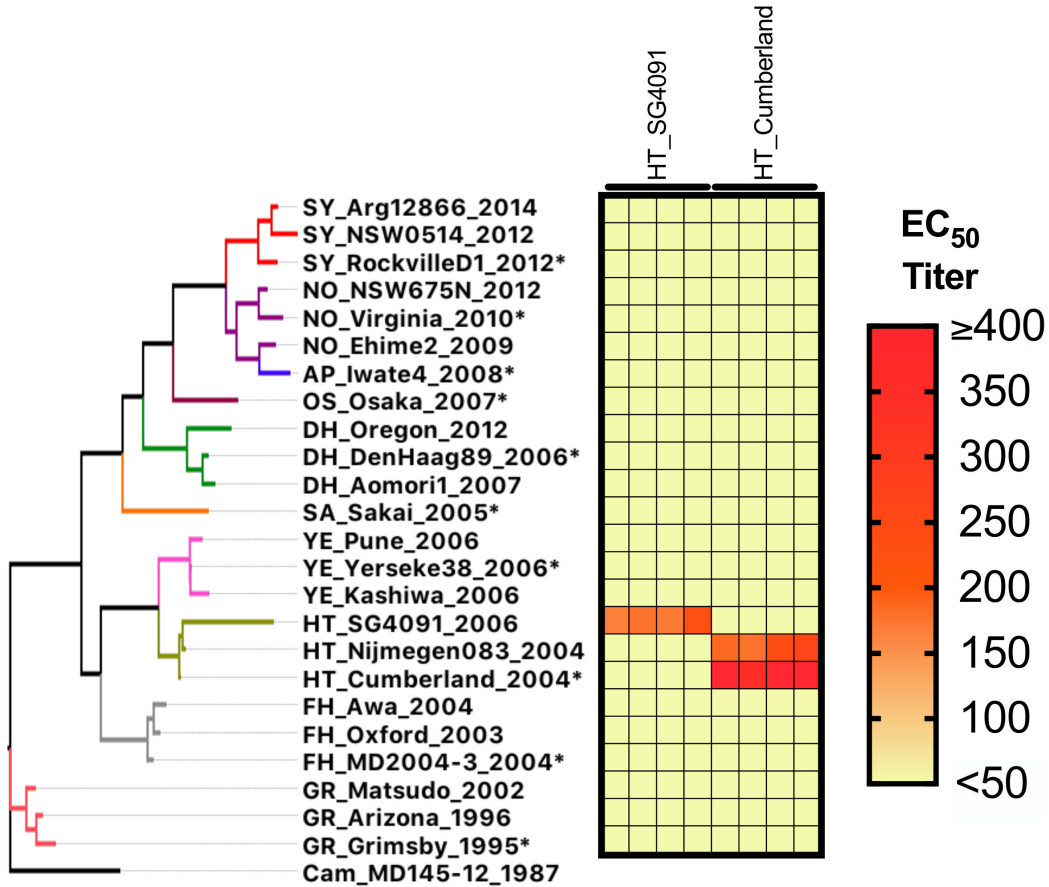


Figure S3. Sera raised against HT_SG4091 2006 exhibits mutually exclusive blockade titers with the predominant Hunter virus. Summary heat map comparing HBGA blockade profiles of murine hyperimmune sera raised for Hunter viruses HT_Cumberland 2004 and HT_SG4091 2006 against representative VLPs. Sera from four mice were used as biological replicates for each VLP and assayed as technical duplicates. Color gradient denotes EC₅₀ blockade titers of each VLP-Sera interaction.

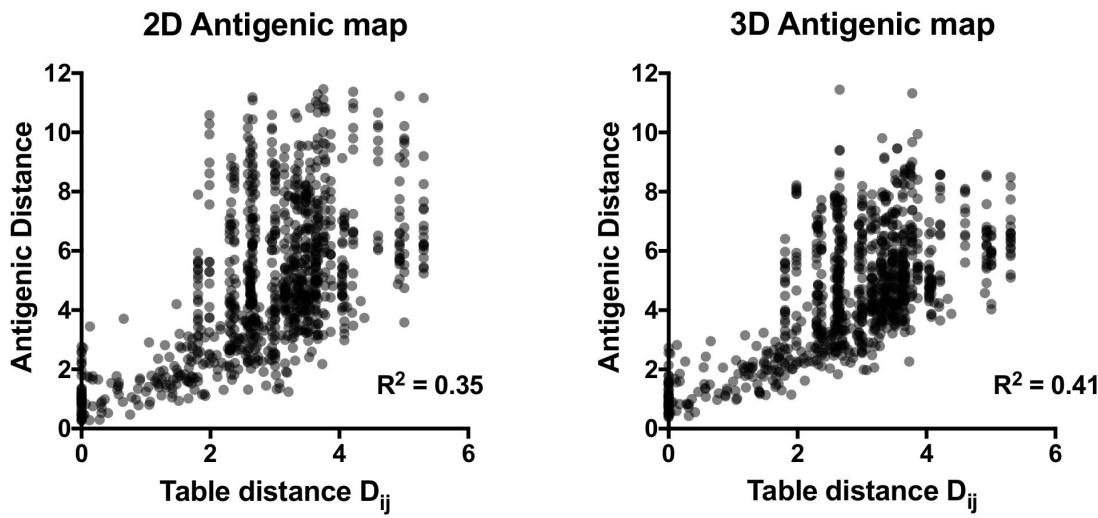


Figure S4. Three-dimensional antigenic cartography of GII.4 noroviruses provides a more precise clustering projection than the two-dimensional analysis. Table vs map distance (i.e. antigenic distance) plots for the 2D (*left*) and 3D (*right*) cartography derived from Fig. 3. R^2 scores from the linear regression models are shown inset on the respective plots.

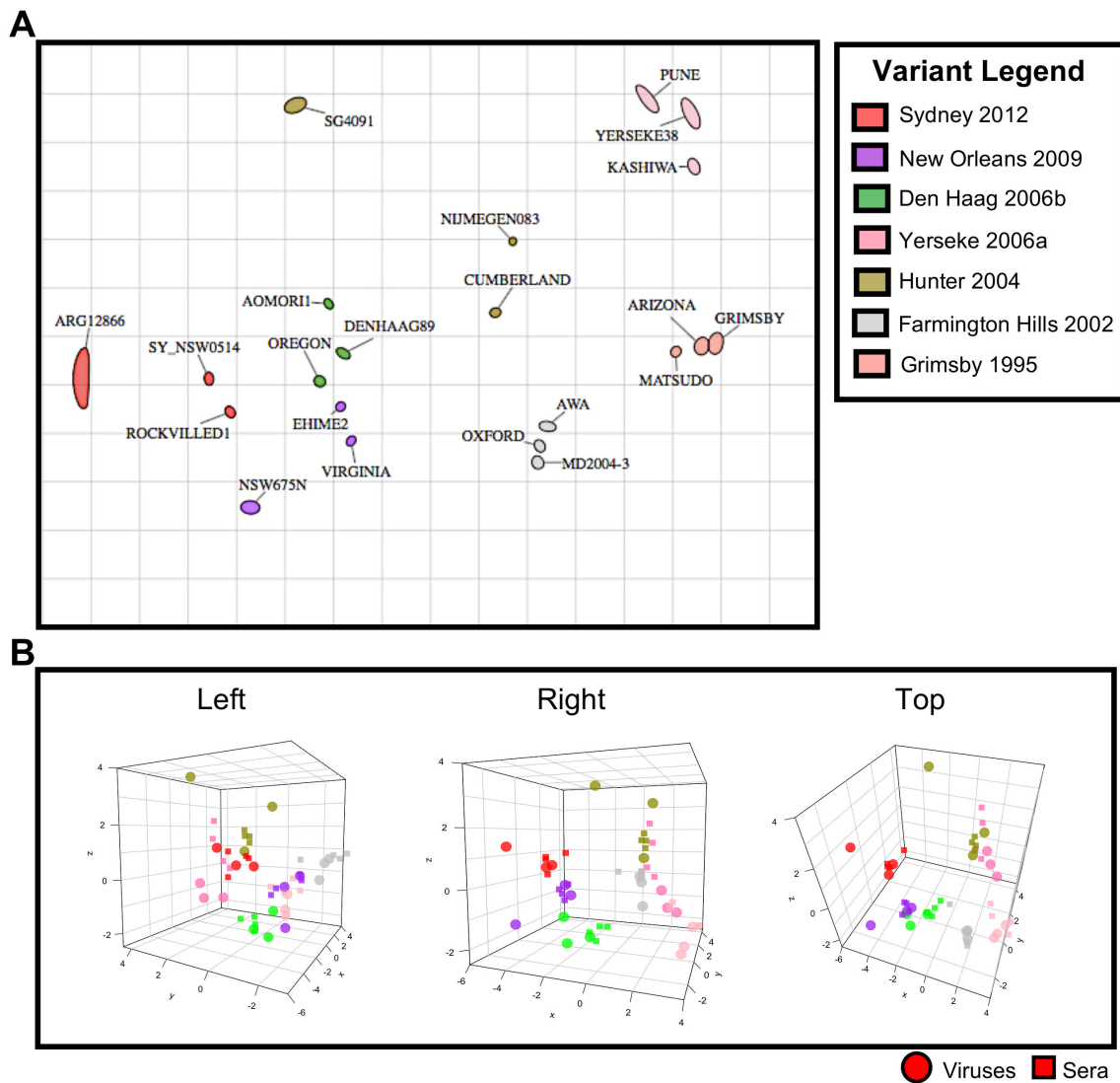


Figure S5. Increased consolidation of GII.4 antigenic cartography clustering trends when minor variant data is omitted. (A) 2D and (B) 3D antigenic cartography projections of representative GII.4 VLPs. VLP and sera data from minor variant viruses SA_Sakai 2005, OS_Osaka 2007, and AP_Iwate4 2008 were omitted. Each unit of antigenic distance (grid lines) denote a two-fold difference in HBGA blockade titers. For visual clarity, the 3D projection is presented at left, right, and top-down angles.

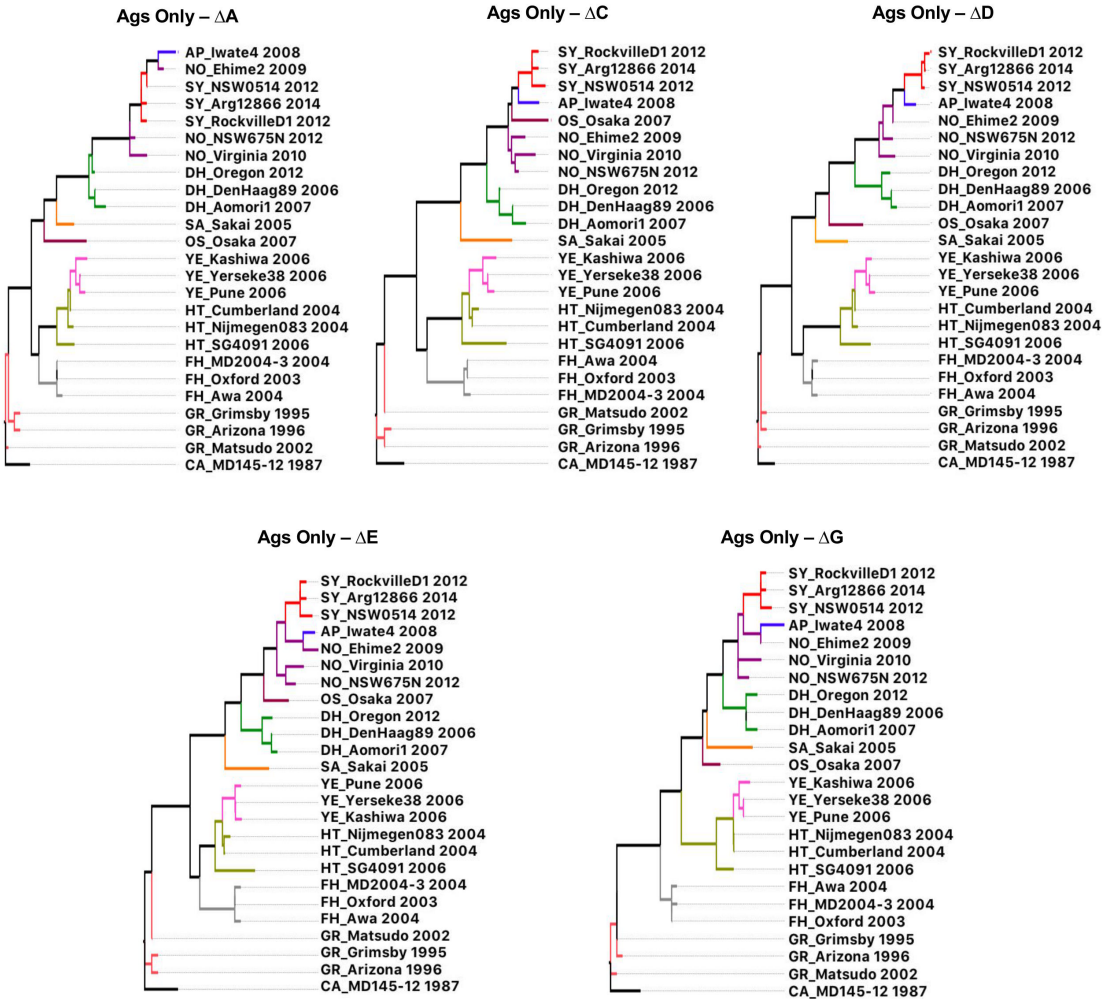


Figure S6. Subtractive analysis on the importance of antigenic sites and GII.4 phylogenetic clustering. Maximum-likelihood phylogenetic trees of representative GII.4 VLPs calculated with only the antigenic site amino acid sequences. The sequences of antigenic sites were systematically removed for the calculation of each respective tree (ΔA , ΔC , ΔD , ΔE , ΔG). Branch length scale is shown below respective trees. Colored branches represent respective variant identities.

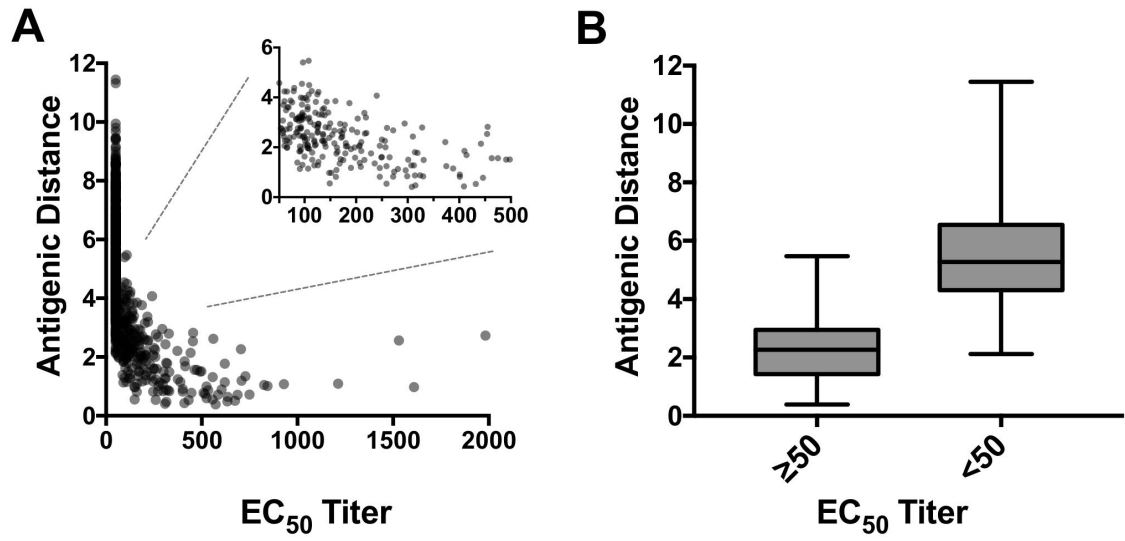


Figure S7. Analysis of the relationship between antigenic distance and EC_{50} titers. (A)

Pairwise analysis of EC_{50} titers (from Fig. 2) plotted against the respective antigenic distance values (from Fig. 3). (*Inset*) Magnified scale of points between EC_{50} titers 50 to 500 for increased visual clarity. **(B)** Statistical analysis of antigenic distances between ≥ 50 and < 50 (detection limit) EC_{50} titers.

Table S1. Nomenclature of GII.4 noroviruses used in this study.

Variant	Virus	Year	Country	Accession
Grimsby 1995 (GR)	Grimsby*	1995	United Kingdom	AJ004864
	Arizona	1996	United States	AF080556
	Matsudo	2002	Japan	AB294778
Farmington Hills 2002 (FH)	MD2004-3*	2004	United States	DQ658413
	Oxford	2003	United Kingdom	AY588022
	Awa	2004	Japan	AB294781
Hunter 2004 (HT)	Cumberland*	2004	United States	EU078414
	Nijmegen083	2004	Netherlands	AB303941
	SG4091	2006	Singapore	JX459599
Yerseke 2006a (YE)	Kashiwa	2006	Japan	AB294789
	Yerseke38*	2006	Netherlands	EF126963
	Pune	2006	India	EU921348
Sakai 2003 (SA)	Sakai*	2005	Japan	AB220922
Den Haag 2006b (DH)	Aomori1	2007	Japan	AB541218
	DenHaag89*	2006	Netherlands	EF126965
	Oregon	2012	United States	KX354081
Osaka 2007 (OS)	Osaka*	2007	Japan	AB434770
New Orleans 2009 (NO)	Virginia*	2010	United States	KX353958
	NSW675N	2012	Australia	KF060086
	Ehime2	2009	Japan	AB933752
Apeldoorn 2007 (AP)	Iwate4*	2008	Japan	AB541274
Sydney 2012 (SY)	RockvilleD1*	2012	United States	KY424328
	NSW0514	2012	Australia	JX459908
	Arg12866	2014	Argentina	MW305623

* Viruses representing predominant sequence for each given GII.4 variant

Movie S1. Animated three-dimensional antigenic cartography of GII.4 noroviruses shows full context of clustering. Animated 3D antigenic map of GII.4 norovirus VLPs derived from EC₅₀ blockade titers against hyperimmune sera. Each unit of antigenic distance denotes a two-fold difference in HBGA blockade titers. GII.4 viruses are represented as large spheres while sera are shown as small cubes. Color denotes respective variant of each VLP.

Dataset S1. Summary of EC₅₀ titers from HBGA blocking experiments. Spreadsheet listing EC₅₀ blockade titers of hyperimmune mouse sera (*bold, top two rows*) against the experimental GII.4 VLP panel (*bold, leftmost column*). Column subheadings M1-M4 denote unique biological replicates of hyperimmune mouse sera raised against the respective GII.4 virus. EC₅₀ titers below the limit of detection have been assigned the values of “<50”.